Indian Journal of Science and Technology, Vol 8(12), DOI: 10.17485/ijst/2015/v8i12/31943, June 2015
ISSN (Print) : 0974-6846
ISSN (Online) : 0974-5645

Quantitative and Qualitative Evaluations of Defect Images in Different Regions of Myocardial Phantom under Implementation of Various Filters in SPECT

Alireza Sadremomtaz* **and Payvand Taherparvar**

Physics Department, University of Guilan, Namjoo Street, PO Box 41365-1159, Rasht, Iran;
sadremomtaz@yahoo.co.uk; p.taherparvar@gmail.com

Abstract

In myocardial perfusion single Photon Emission Computed Tomography (SPECT), images are degraded by photon attenuation, distance-dependent collimator, detector response. The filters in reconstruction process can greatly affect the quality of the SPECT images. The purpose of this study is to make quantitative and qualitative evaluation of the acquired SPECT images of similar defects which are located in the different regions of myocardial phantom under implementation of different filters. Herein, rectangular defects with the same thickness were inserted on the different regions of on the inner wall of the myocardial phantom. Myocardial perfusion study was performed with meta-stable Technetium with a dual head SPECT system. Raw data was reconstructed by filter back projection method with some filters. Then, results of implementation of various filters with different parameters on the contrast, signal to noise ratio and size of defects images in transverse, coronal and sagittal views of the phantom have been studied. The results show that contrast, signal to noise ratio and size of defects images are depending on the defect locations, type of filters and the selection of view which is examined for specified defect.

Keywords: Filter, Myocardial Phantom, SPECT

1. Introduction

Single Photon Emission Computed Tomography or SPECT has considerably improved myocardial image contrast and quality and led to improvement in ability to detect coronary artery disease and particularly to assess its severity[1,2]. However, myocardial perfusion quantitation remains an elusive goal due to the biological limitations of tracers, photon scattering and partial volume effect[3]. This makes absolute or even relative quantitation of the tracer concentration distribution in the myocardium difficult in the clinical setting[4]. On the other hand, despite of the developing new techniques of image reconstruction in SPECT[5–7], Filter Back Projection (FBP) method is still widely used due to its computational efficiency and speed[5,8]. In FBP, compensation of image degradation is done by implementation of different filters in the reconstruction process to enhancement of image quality and noise suppression with keeping of the more image details[9,10]. In this method, using of unsuitable filter may significantly degrade image quality and affect the accuracy of quantitative results[11]. The selection of filter is usually a trade-off between the extent of fine detail reduction and noise suppression as well as the spatial frequency spectrum of the image data of interest[10]. Degree of high frequency reduction could be controlled by selecting a cut-off frequency in filtering process. Indeed, the cut-off frequency determines where the filter rolls off to zero gain. The location of the cut-off frequency specified how the filter will affect both resolution and image noise level.

*Author for correspondence

This study was carried out to show the effect of SPECT filters on the detection capability of reconstructed images of defects, by defining some criteria such as contrast and Signal to Noise Ratio (SNR) as qualitative analysis, in different areas of the myocardial phantom. Furthermore, although cardiac diagnosis does not normally demand absolute quantification of defect size, but, information about these quantities is important for the follow-up of cardiac patients[12]. Thus, the dimension of defect images located in the anterior, septal, infero posterior, lateral and apical regions as quantitative analysis have been calculated in transverse, coronal and sagittal views of three-dimensional image registration of phantom which was reconstructed by different filters.

2. Material and Methods

We built a phantom simulating the myocardial wall of the left ventricle. The phantom consists of 2 concentric cylinders with a half-spherical end cup on each end. At first, for testing of the integrity of the myocardial phantom, it was filled with 1 mCi uniform distribution of meta-stable Technetium-99 (Tc-99m) water solution which is about 20 percent of injected Technetium into patient body in the myocardial SPECT. Then, the phantom was placed on the imaging couch of dual head SPECT system; model ADAC EPIC Vertex, approximately at the center of rotation. To increase the clinical usefulness of SPECT studies, the quality control programs were performed. Imaging has been done with the SPECT system which equipped with Low Energy High Resolution (LEHR) collimator. Acquired images were investigated for certification of the myocardial phantom by nuclear medicine physicians. This phantom was certified as a standard myocardial phantom.

At the next step, five rectangular Plexiglas defects of 20*20 *8mm^3 were inserted at five regions of on the inner wall of the phantom consist of anterior, septal, inferoposterior, lateral and apical regions Figure 1(a). For SPECT studies, the phantom was filled with 1 mCi of Tc-99m water solution. The phantom was placed on the center of imaging couch of SPECT system, so that the long axis made an upward angle of 15° with the couch surface. Imaging has been done with the SPECT system equipped with Low-Energy High-Resolution (LEHR) collimator. The imaging protocol was considered as follows: rotation radius 20 cm, rotation angle of 360˚, using of the LEHR collimator and consisting of 64 views of 20 seconds. Step-and-shoot mood, and zoom factor of 2 were used too. Then, the raw binary data was transferred to the PC and was decoded by use of the some script were written in MATLAB software. Furthermore, some scripts were also written in the MATLAB to reconstruct the raw data using FBP method by implementation of Hann, Hamming, Butterworth, Cosine and Shepp-Logan filters. Values of 0.2 to 0.9 were allocated for the cut-off frequency of the Hann, Hamming, Cosine and Shepp-Logan filters. And so, the Butterworth filter, which is a Band-Pass filter with two adjustable parameters of cut-off frequency and order, was used with the values of 0.2 to 0.9 for cut-off frequency and order of 9. The one slice of transverse, coronal and sagittal views of phantom which defects are clearly detected is represented in Figure 1 (b), (c), and (d), respectively.

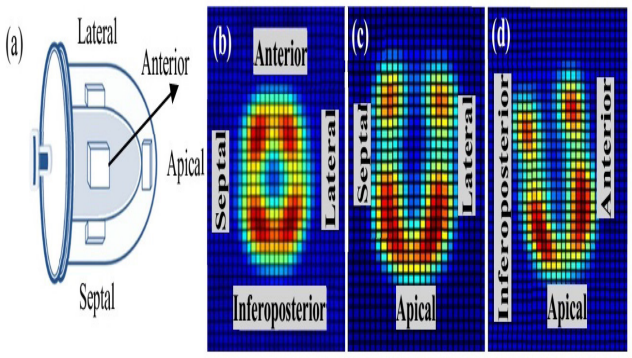

Figure 1. (a) Locations of defects inside schematic diagram of myocardial phantom, (b) Transverse (c) Coronal and (d) Sagittal view of SPECT images of phantom.

2.1 Calculation of Contrast, Signal-to-Noise Ratio and Defect Size

We draw some Regions Of Interest (ROIs) through the defect locations from the normal myocardium to defect region and further in the transverse, coronal and sagittal views of phantom image in the MATLAM environment. The MATLAB software provides us with information including line profile, mean count, maximum and minimum count and number of counts in any ROI. For each ROI, we measure the maximum count in normal myocardium ($N_{max(myo)}$), minimum count in defect ($N_{min(def)}$), and minimum count in background (heart hole region) ($N_{min(hole)}$). Because of the different attenuation in each direction of defect in the normal myocardium, the peaks

at the two sides of it are not equal. Two Gaussian functions were fitted on the generated data related to the peak locations, which were obtained from the line profiles. Then the number of pixel between the smaller peak and the steep of the other peak having same count (N_{pixel}) was calculated by MATLAB software. Finally, by using all of these measurements, the maximum contrast, Signal-to-Noise Ratio (SNR), and defect size were calculated as follow:

$$Max.Contrast = (N_{\max(myo)} - N_{\min(def)}) / N_{\max(myo)} \quad (1)$$

$$SNR = (N_{\max(myo)} - N_{\min(def)}) / N_{\min(hole)} \quad (2)$$

$$Defect.Size = N_{pixel} \times 3mm \quad (3)$$

Where, 3mm is a pixel size.

3. Results

3.1 Transverse View

The one slice of transverse view which four defects are detected is represented in Figure1 (b).

3.1.1 Defect in the Septal Region

The results of estimating the size of defect in the septal region [detected defect in the left side of Figure 1 (b)] versus cut-off frequency for different filters has been shown in Figure 2 (a). The results show that with increasing of the cut-off frequency, calculated defect size is generally enlarging. Prominently point in this diagram is less variation in apparent dimensions of defect image under implementation of the Butterworth and Shepp-Logan filters in comparison with the other filters.

The contrast calculation of defect image for all filters show that the best results for the contrast could be achieved by implementation of the Butterworth and Shepp-Logan filters, as shown in Figure 2 (b), respectively. These values were obtained at the highest value of the cut-off frequency. In addition to, another advantage of the Butterworth and Shepp-Logan filters is that they have less variation for the different values of the cut-off frequency larger than 0.3.

Increasing curve for SNR diagrams belong to the Hann, Hamming, Cosine and Shepp-Logan filters, as shown in Figure 2 (c), are appeared. Excellence result

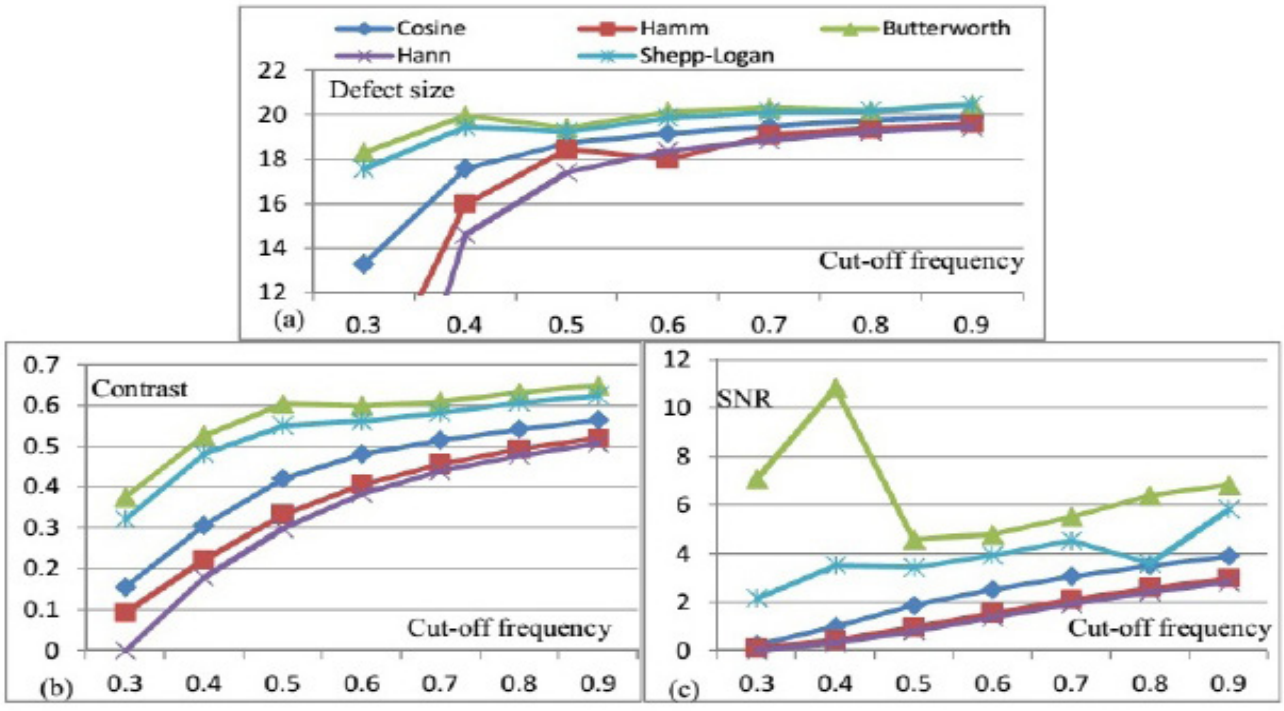

Figure 2. Diagram of defect size (mm) (a) . contrast (b) and SNR (c) vs. cut-off frequency for the Hann x, Hamming ■ Cosine ♦, Butteworth ▲ and SheppLogan ✳ fillters for the septa1 defect in the transverse view.

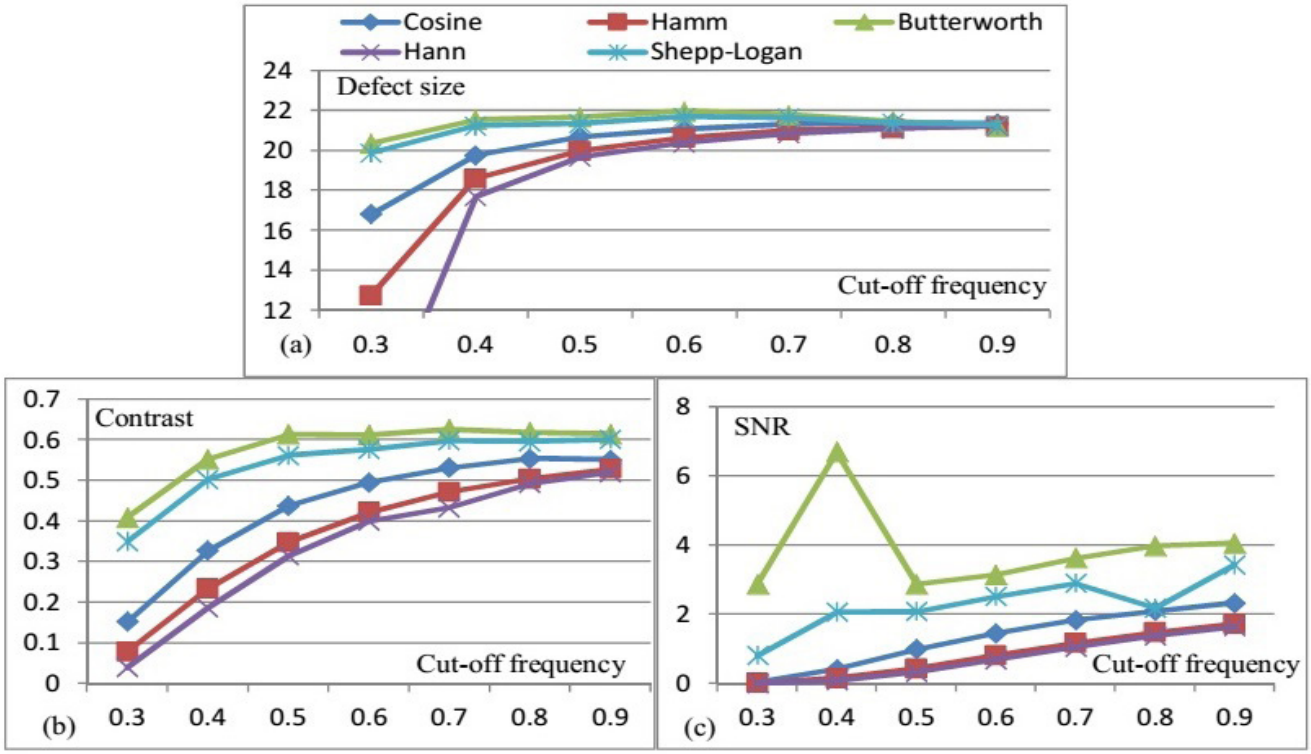

Figure 3. Diagram of defect size (mm) (a) , contrast (b) and SNR (c) vs. cut-off frequency for the Hann x, Hamming ■Cosine ♦, Butterworth ▲ and SheppLogan ✳ fillters for the lateral defect in the transverse view.

belong to the Butterworth filter with the cut-off frequency of 0.4 are quite apparent.

3.1.2 Defect in the Lateral Region

The results of calculated defect size in the septal region [detected defect in the right side of Figure 1(b)] for various filters - Figure 3(a) - are resemble to the results of the septal defect, but defect dimension usually appears larger than its actual size in Figure 3(a).

Results of the contrast of defect images in Figure 3(b) are the same as later, but the results of Butterworth filter are almost constant for values of the cut-off frequency larger than 0.4. The diagrams of SNR of defect images are similar to the SNR diagram belongs to the lateral defect images (Figure 3(c)), but the results are worth than later, to some extent.

3.1.3 Defect in the Infer Posterior Region

The results of estimating the size of defect in the infer posterior region [bottom detected defect in Figure 2(a)] in all cases show that approximated defect size seems less than its actual dimension in Figure 4(a). With increasing of the cut-off frequency for the Hann, Hamming and Cosine filters, these estimated dimensions close to the actual size, but never reach to it. The diagrams related to the Butterworth and Shepp-Logan filters are resemble to each other and different from other filters. The best result for defect dimension is achieved by use of the Butterworth and Shepp-Logan filters with the cut-off frequency of 0.4 that is about 19.86 mm.

The obtained results for the contrast of defect image as shown in Figure 4(b) are same as later except that the Butterworth filter with cut-off frequency of 0.7 could produce the best result, and then, the better results for other filters is attainable by use of the cut-off frequency of 0.9. Totally, calculated contrast for image of the infer posterior defect is less than obtained results for the defects in the lateral and septal regions.

The results of the SNR of this defect image, as shown in Figure 4(c), is same as SNR results related to the defect in the other regions, but the results belong to the Butterworth filer are weaker than others. The best result for the SNR of defect detection is achieved by use of the Butterworth filter with the cut-off frequency of 0.4.

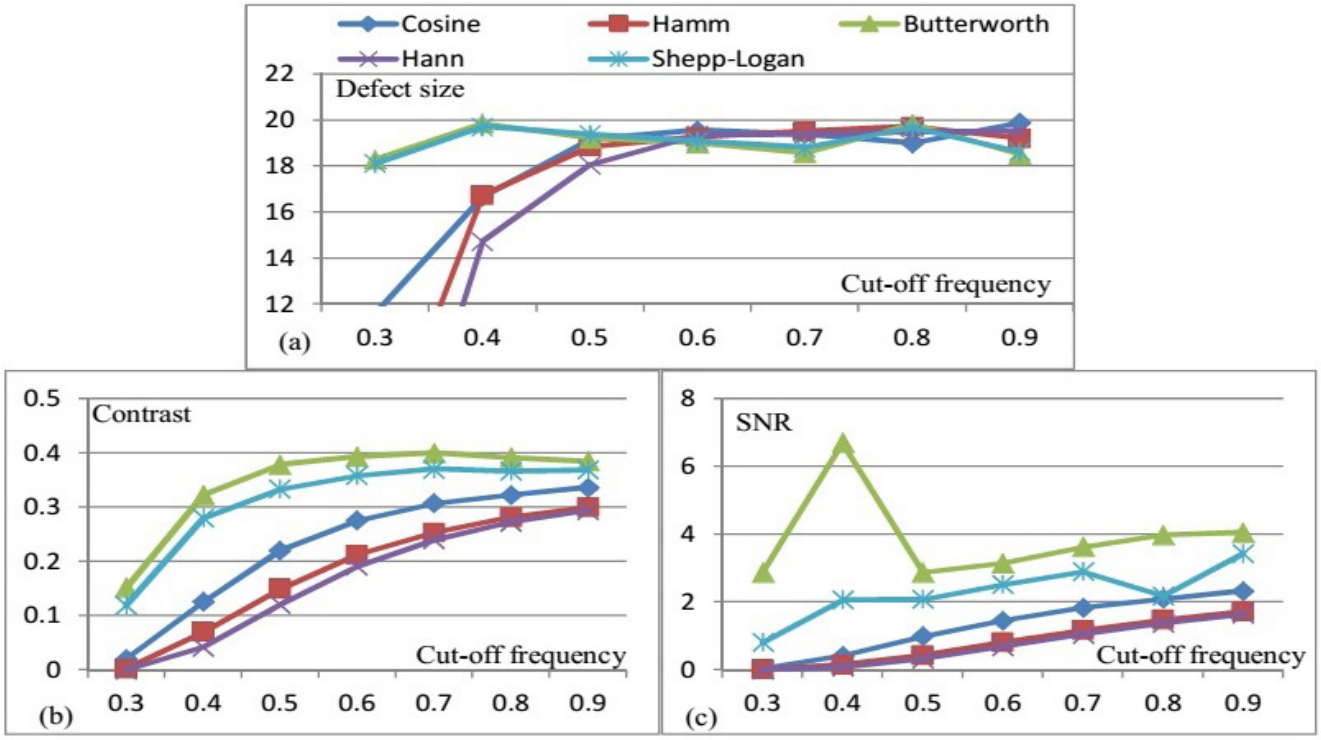

Figure 4. Diagram of defect size (mm) (a) , contrast (b) and SNR (c) vs. cut-off frequency for the Hann x, Hamming ■Cosine ◆, Butteworth ▲ and SheppLogan ✱ fillters for the inferoposterior defect in the transverse view.

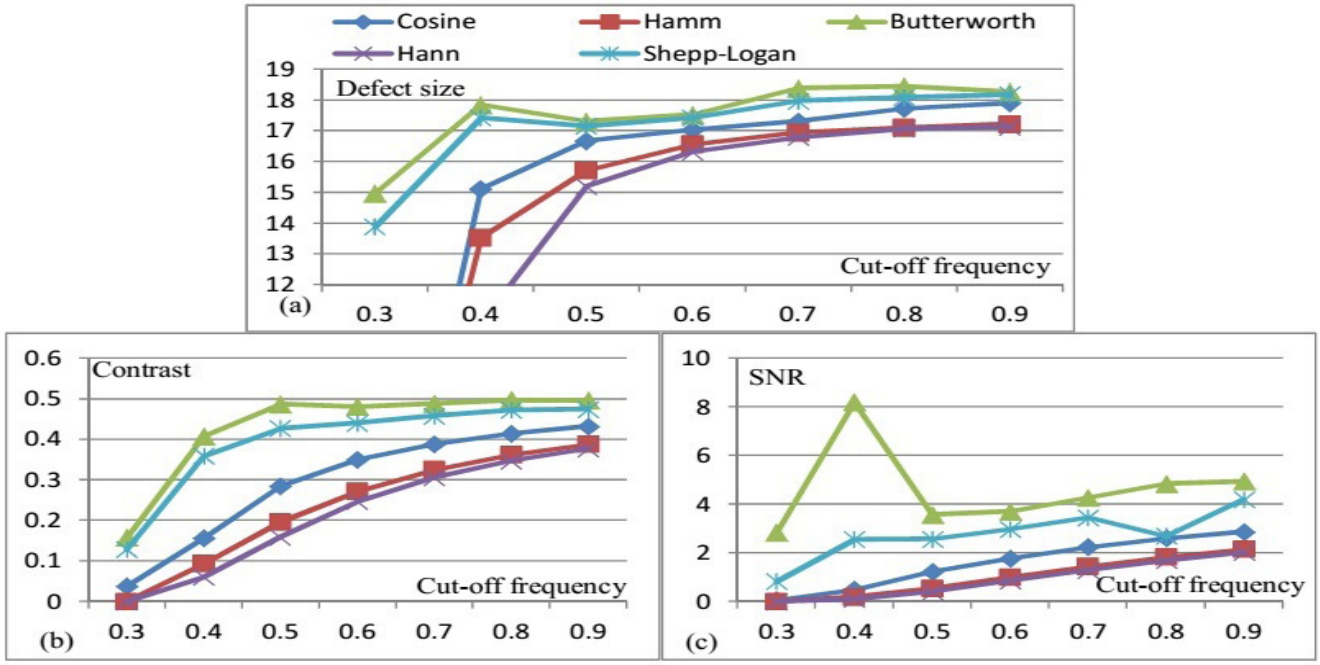

Figure 5. Diagram of defect size (mm) (a) , contrast (b) and SNR (c) vs. cut-off frequency for the Hann x, Hamming ■Cosine ◆, Butteworth ▲ and SheppLogan ✱ fillters for the anterior defect in the transverse view.

3.1.4 Defect in the Anterior Region

Results of the size of defect in the anterior region [detected defect in the up side of the Figure 1(b)] could be seen in Figure 5(a). The represented diagram for the defect size show that the best results for the Shepp-Logan, Cosine, Hann and Hamming filters are achieved by use of the cut-off frequency of 0.9, but the best result for defect dimension is obtained by use of the Butterworth filter with cut-off frequency of 0.8 that is about 18.45 mm. Unlike obtained results for defect size in the septal and lateral regions, the calculated defect size for defect in the anterior region is always less than the actual dimension.

Results of the contrast and SNR of the anterior defect versus the cut-off frequency have been shown in Figure 5(b) and (c), respectively. The contrast results show the same behavior for implementation of Hann, Hamming, Cosine and Shepp-Logan filters in the reconstruction process of phantom image. Excellence of the Butterworth filter in this diagram is apparent, and the best result for this filter is achieved in the wide range of the cut-off frequency (≥0.4). The SNR results, as shown in the Figure 5(c), are the same as calculated SNR of inferoposteriordefect image, but these results are better than it.

3.2 Coronal View

The one slice of coronal view which three defects are clearly detected is represented in Figure 1(c). Left, right and bottom detected defects in this figure is related to defects in the septal, lateral and apical regions, respectively.

3.2.1 Defect in the Septal Region in the Coronal View

The results of estimating the size of the defect in the septal region [left detected defect in Figure 1(c)], as shown in Figure 6(a), show that the calculated defect dimension is always larger than actual size and theses values increase with increasing of the cut-off frequency. The best result is achieved by use of the Hann and Butterworth filters with the cut-off frequency of 0.3. The contrast and SNR results in Figures 6(b) and (c) show the superiority of the Butterworth filter as later, especially in the SNR diagram.

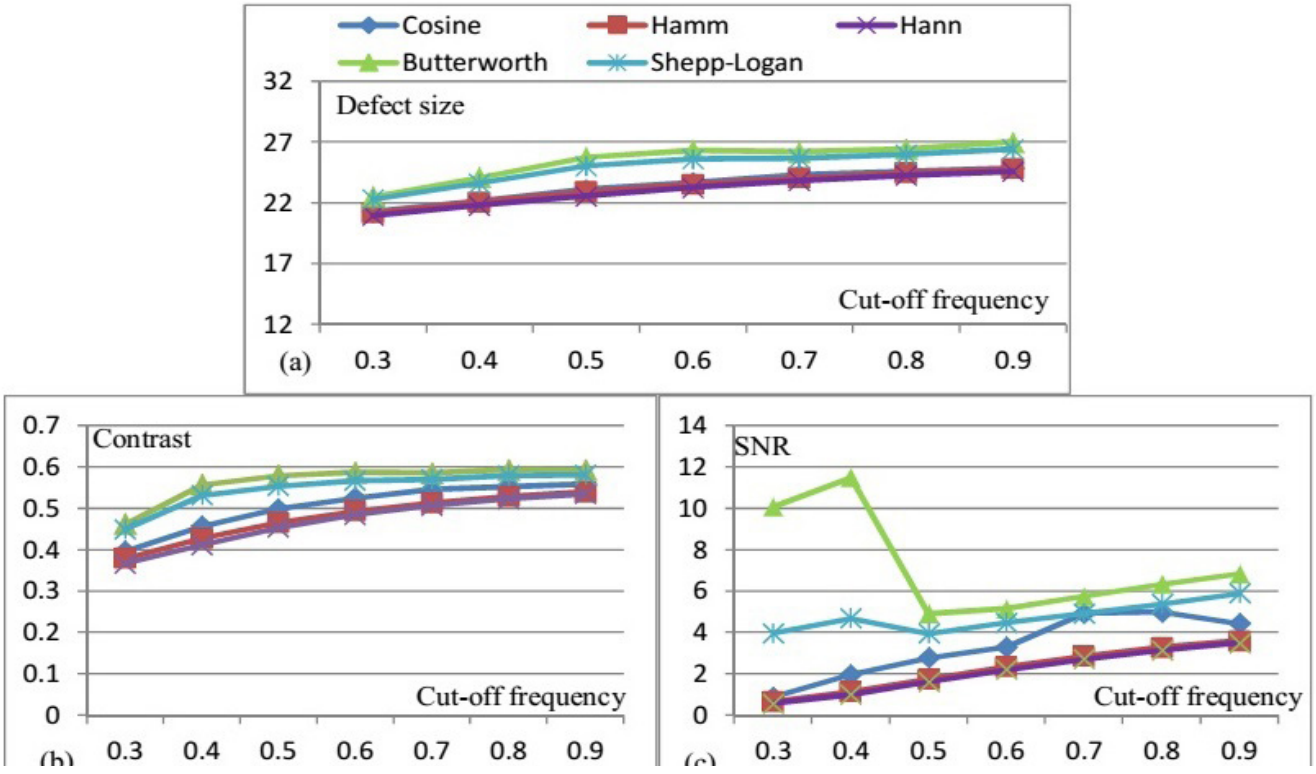

Figure 6. Diagram of defect size (mm) (a) , contrast (b) and SNR (c) vs. cut-off frequency for the Hann x, Hamming Cosine , Butteworth and SheppLogan fillters for the septal defect in the coronal view.

The results of the contrast and SNR of reconstructed image of septal defect by implementation of the Shepp-Logan filter are interesting.

3.2.2 Defect in the Lateral Region

The results of calculating size of defect in the lateral region [right detected defect in Figure 1(c)] versus cut-off frequency are represented in Figure 7(a). Unlike the former, the apparent defect size decreases and becomes closer to the actual value, with increasing of the cut-off frequency in the diagrams related to the Butterworth and Shepp-Logan filters. On the other hand, variation in the estimated dimensions of the defect in comparison with the cut-off frequency for diagrams belong to the Cosine, Hann and Hamming filters are negligible. The best result is related to the Butterworth filter with the cut-off frequency of 0.9.

Results of contrast and SNR diagrams of the lateral defect detection, as shown in Figures 7(b) and c, are very similar to the results belong to the septal defect. The best results could be achieved by implementation of the Butterworth filter with cut-off frequency of 0.4.

3.2.3 Defect in the Apical Region

Unlike the calculated dimensions of defect in the right and left sides of the coronal view (lateral and septal regions), which seem larger than actual size, estimation of the defect size in the apical region [bottom detected defect in the Figure 1(c)] appears much smaller than actual as illustrated in Figure 8(a). Defect size at best value could be estimated about 17.48 mm at the cut-off frequency of 0.4 by implementation of the Butterworth filter.

Diagrams related to the contrast and SNR of the apical defect in the coronal view of myocardial phantom are shown in Figure 8(b) and (c), respectively. The results indicate that the Butterworth filter with the cut-off frequency of 0.4 is produced the best outcome. Interestingly point for the Butterworth filter is that for the values of cut-off frequency larger than 0.3, the worst results related to this filter is always better than others. After the Butterworth filter, the Shepp-Logan, Cosine, Hann and Hamming filters produce better results, respectively. Moreover, increasing behavior of curves related to the last three filters will lead to improvement of the contrast results. Thus, in the coronal images, not only diagnosis of

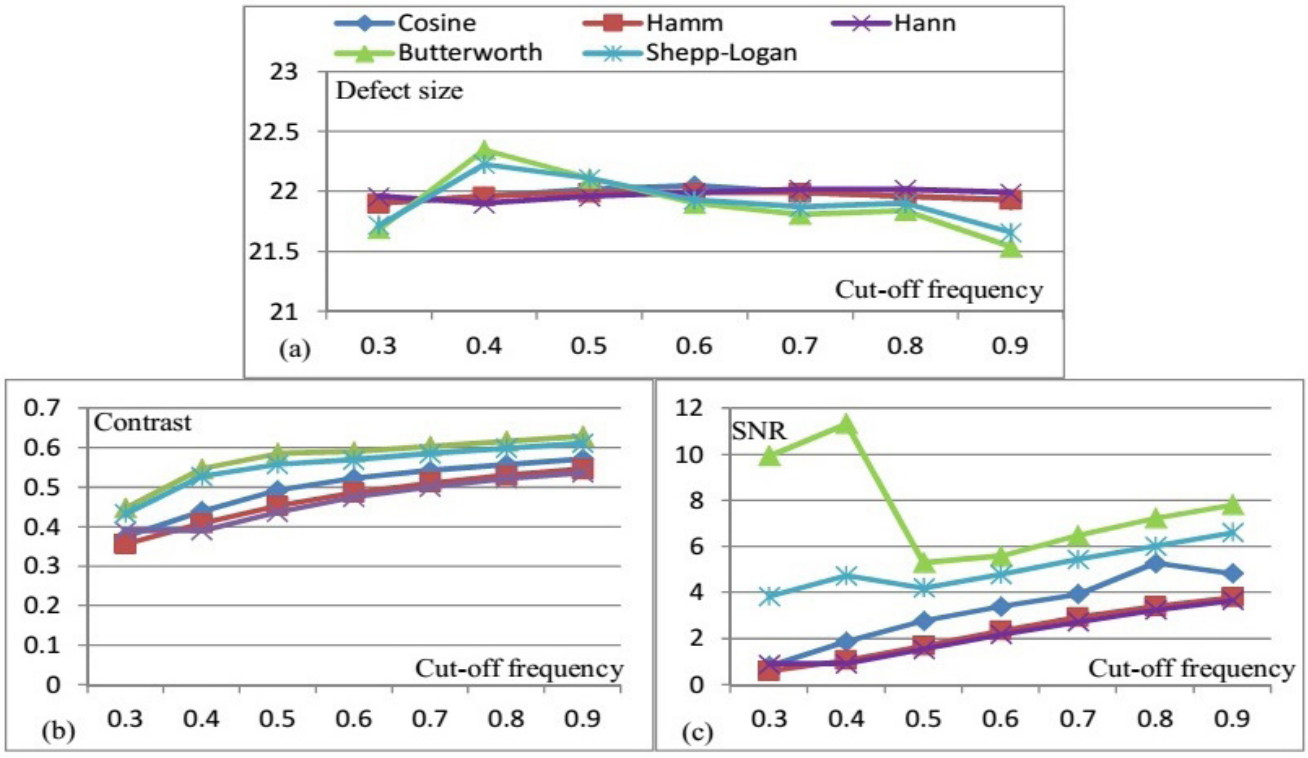

Figure 7. Diagram of defect size (mm) (a) , contrast (b) and SNR (c) vs. cut-off frequency for the Hann x, Hamming ■ Cosine ♦, Butteworth ▲ and SheppLogan ✳ fillters for the lateral defect in the coronal view.

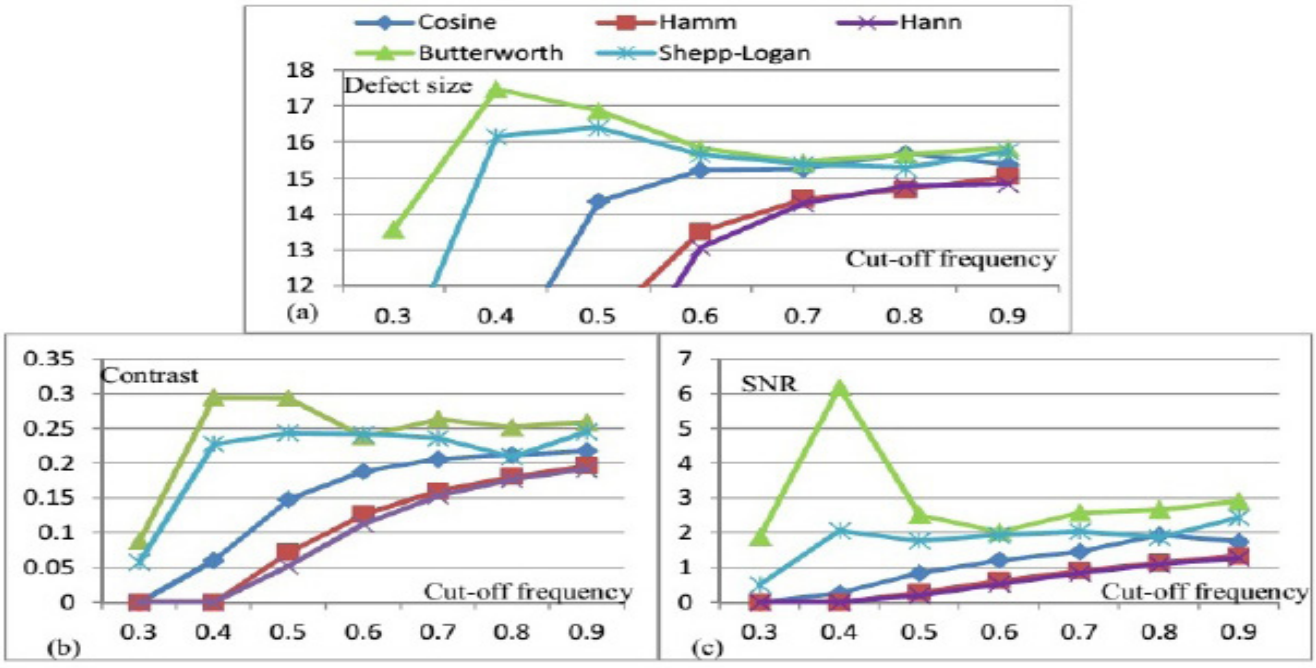

Figure 8. Diagram of defect size (mm) (a) , contrast (b) and SNR (c) vs. cut-off frequency for the Hann x, Hamming Cosine , Butteworth and SheppLogan fillters for the apical defect in the coronal view.

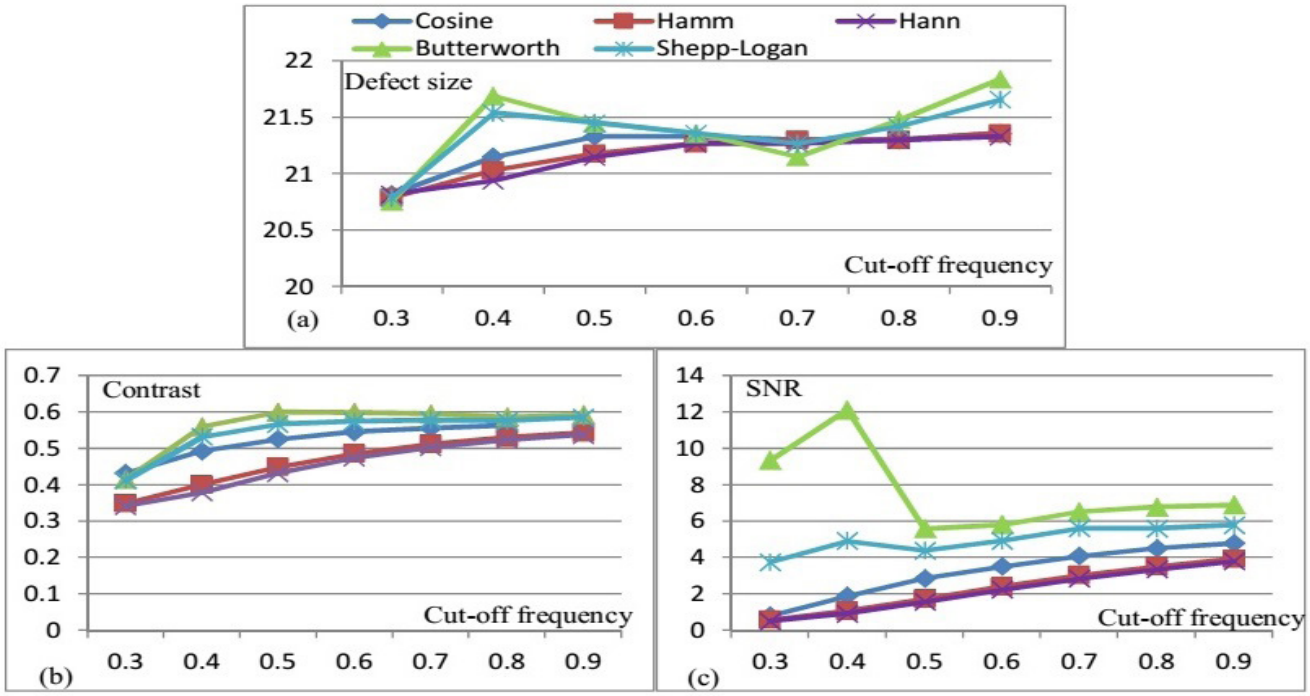

Figure 9. Diagram of defect size (mm) (a) , contrast (b) and SNR (c) vs. cut-off frequency for the Hann x, Hamming Cosine , Butteworth and SheppLogan fillters for the anterior defect in the sagittal view.

defect in the apical region will be more difficult, but also defect size is estimated less than the actual dimension.

3.3 Sagittal View

The one slice of the sagittal view which three defects are clearly detected is represented in Figure 1(d). Right, left and bottom detected defects in this figure is related to defects in the anterior, infer posterior and apical regions of the myocardial phantom, respectively.

3.3.1 Defect in the Anterior Region

The results of estimating the defect size in the anterior region [right detected defect in the Figure 1(d)] in Figure 9(a) show that calculated dimensions is always larger than the actual amount and estimated size usually increases with increasing of the cut-off frequency for curves related to the Hann, Hamming and Cosine filters. Same behavior of curves related to the Butterworth and Shepp-Logan filters in this diagram could be observed.

The contrast and SNR results, as shown in Figure 9(b) and (c), show the superiority of the Butterworth filter, especially in the SNR diagram. Butterworth filter with cut-off frequencies of 0.5-0.9 and 0.4 produced the best results for the contrast and SNR of anterior defect detection in the sagittal view, respectively. The variation of the cut-off frequency for this filter, especially values larger than 0.4, has less effect on the contrast value of image of inferoposterior defect.

Although, the best result for the estimation of the defect size could be produced by use of the lowest value of the cut-off frequency, but the worst results for the contrast of defect detection are produced in this situation.

3.3.2 Defect in the Infer Posterior Region

Results of estimating the size of infer posterior defect [left detected defect in Figure 1(d)] for different filters versus cut-off frequency. Figure 10(a) show that calculated defect dimension is always larger than actual amount and these values often increase with increasing of the cut-off frequency. Thus, more correct estimation of the defect size is usually possible in lower values of the cut-off frequency. The curves related to the Hamming, Hann and

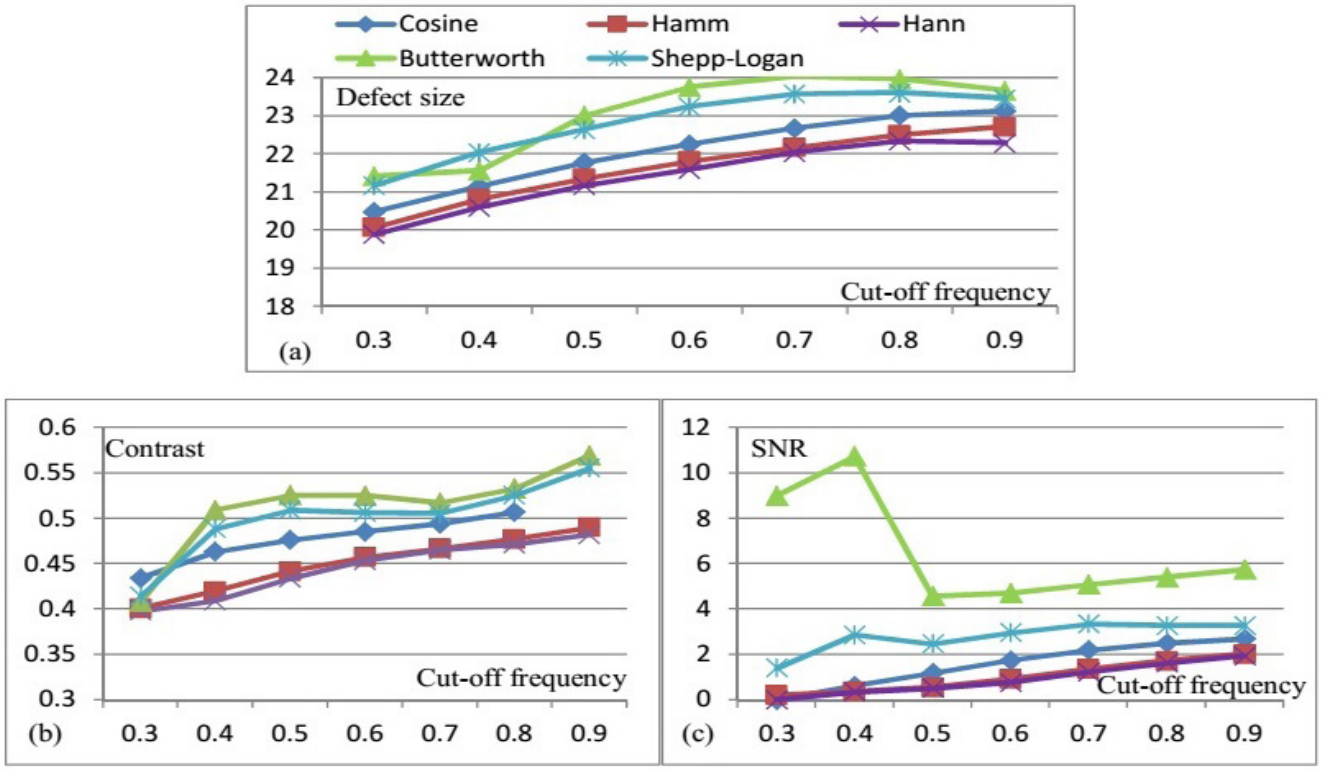

Figure 10. Diagram of defect size (mm) (a) , contrast (b) and SNR (c) vs. cut-off frequency for the Hann x, Hamming Cosine , Butteworth and SheppLogan fillters for the inferoposterior defect in the sagittal view.

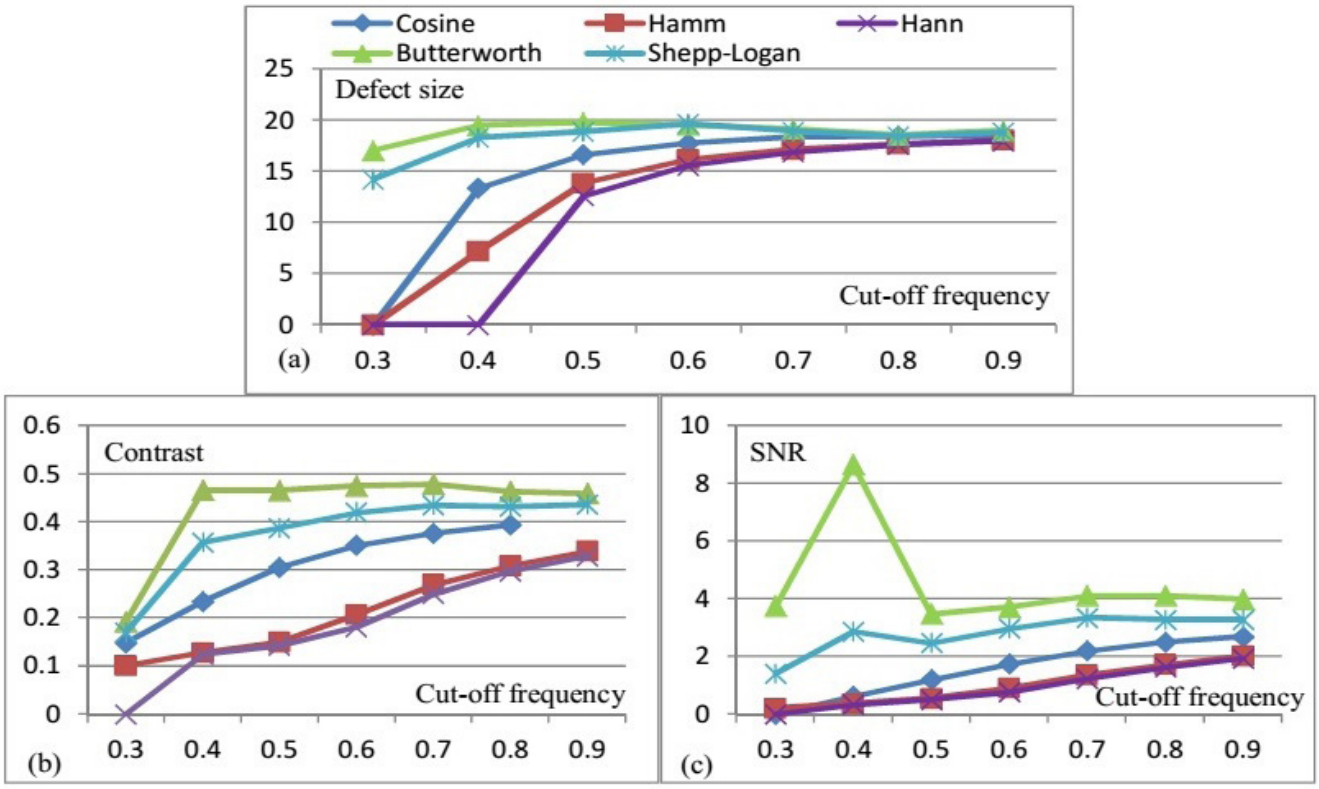

Figure 11. Diagram of defect size (mm) (a) , contrast (b) and SNR (c) vs. cut-off frequency for the Hann x, Hamming ■ Cosine ♦, Butteworth ▲ and SheppLogan ✱ fillters for the apical defect in the sagittal view.

Cosine filters have the same behavior and the accurate result is achieved by use of the Hamming filter with the cut-off frequency of 0.3 which is about 19.89mm.

The results of the contrast and SNR of this defect detection [Figures 10(b) and (c)] show the excellence of the Butterworth filter. The best values of SNR and contrast of the defect image could be produced by use of the Butterworth filter with cut-off frequencies of 0.9 and 0.4, respectively.

3.3.3 Defect in the Apical Region

The results of estimating the size of defect in the apical region (bottom detected defect in the Figure 1(d)) under implementation of different filters versus the cut-off frequency are represented in Figure 11(a). Reverse behavior of represented curves for the Butterworth and Shepp-Logan filters which have decreasing function with a slight slope, in comparison with the Cosine, Hann and Hamming filters, which have increasing function, is quite evident. Better precision in the estimating of the apical defect size is attainable by implementation of the Butterworth filter with cut-off frequency of 0.5 [Figure 11(a)].

Diagrams related to the contrast of this defect detection by implementation of different filters, as shown in Figure 11(b), imply that the curve belongs to the Butterworth filter could be produced better results than others and the best result could be obtained by used of the cut-off frequency of 0.4. And so, with increasing of the cut-off frequency, contrast values will not change significantly. After the Butterworth filter, results related to the Shepp-Logan, Cosine, Hann and Hamming filters is better, respectively. Moreover, increasing functions related to the curves belong to the last four filters will lead to the better results.

The results of the SNR of this defect image [Figures 11(c)] also show the advantage of the Butterworth and Shepp-Logan filters, respectively. As before, the best value of the SNR of the defect image could be produced by use of the Butterworth filter with the cut-off frequency of 0.4.

4. Conclusion

The results of the transverse view of myocardial phantom show that the detection capability of the lateral and septal defects are similar to some extent, because of the symmetry of defects position with regard to the rotation of the camera head in SPECT system. In this view, the contrast and SNR results of the inferoposterior defect image are worse than others, which can be related to the defect position in the bottom side of the myocardial phantom in adjacent of the SPECT couch. Therefore, diagnosis of the defect in the inferoposterior region is more ambiguous than lateral, septal and anterior defects. In this view, the dimensions of the defects could be estimated with a good approximation by use of the specified parameters for different filter, especially for Butterworth filter.

Results of detected defects in the lateral and septal regions in the coronal view, which also are seemed in the transverse view, show that the best results for defect size accuracy are achieved by use of the transverse view. However, the SNR results of lateral defect show the excellence of the coronal view.

Results of detected defects in the anterior region of phantom in the transverse view, which also appear in the right side of the sagittal view, show that the defect dimension always seem smaller than actual size in the transverse and larger in the sagittal view. But, for this defect the results belong to the sagittal view are more consistent with actual dimension. And so, the better results for the contrast and SNR of this defect could be achieved by use of the sagittal view.

Results of detected defects in the inferoposterior region of phantom in the transverse view, which also appear in the left side of the sagittal view, show that the defect dimension always seems smaller than actual size in the transverse view, whereas it appears larger than actual dimension in the sagittal view. In addition to, the better results for the contrast and SNR calculation of this defect could be achieved by use of the sagittal view.

Our investigation for defect in the apical region, which could be seen in the bottom regions of the sagittal and coronal views, show that detection of this defect is very difficult for reconstructed image by use of the Hann, Hamming and Cosine filters with the values of the cut-off frequency lower than 0.6. However, Butterworth filter is the best choice for its diagnosis. For this defect, the sagittal view not only could show this defect image with better contrast and SNR, but also it could estimate its size with a small error. Totally, diagnosis of apical defect will be more difficult than others due to surrounding of the whole lateral surfaces of the defect by the greater volume of radioactive solution and locating along the end side of the inner tube of the myocardial phantom.

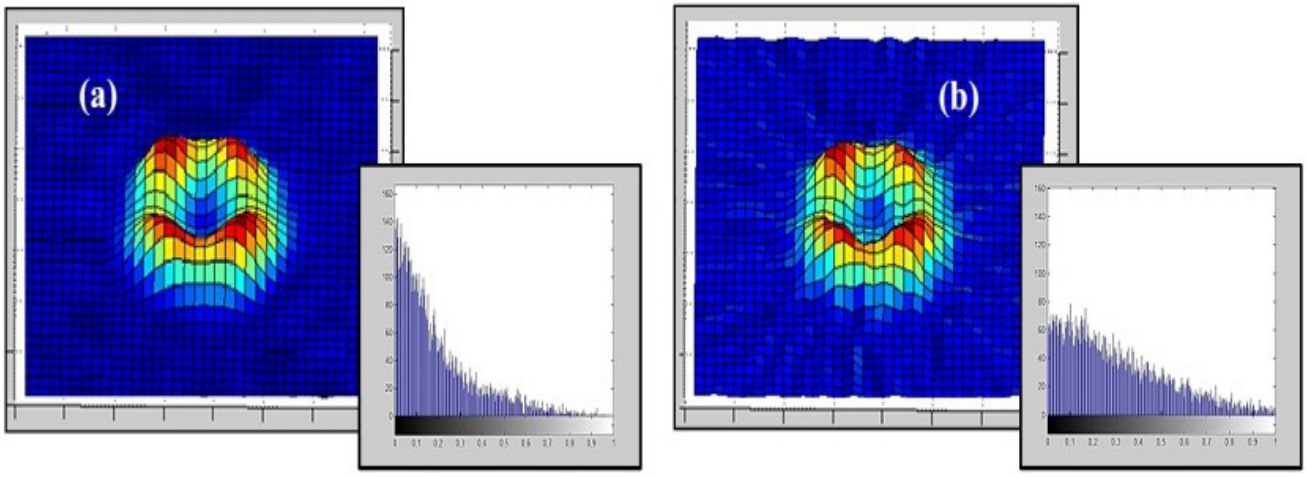

Figure 12. Example of three-dimensional shaded surface of transverse of myocardial phantom reconstructed by Butterworth filter with the cut-off frequenies of 0.4 (a) and 0.9 (b) with theirs histogram diagrams

Until now, calculation of the contrast, SNR and size of defects images almost indicate the Butterworth filter with cut-off frequencies of 0.4 and 0.9 give the best results.

Visual examination of these results can be done by use of the Figure 10 that related to transverse view of image phantom reconstructed by Butterworth filters with cut-off frequencies of 0.4 and 0.9 with their histogram diagrams. Inspection of this figures with their histogram show that smoother image with better contrast could be produced by use of the cut-off frequency of 0.4. Indeed, using lower values of the cut-off frequency cause suppressing signals with high spatial frequencies that dominated by noise. Although removing high frequency will be suppressed with a chance of losing some useful signal, but it doesn't extremely effect on the defect detectability and images details, in this situation. Increasing of the cut-off frequency up to 0.9 can preserve the resolution, but does not suppress noise sufficiently.

5. Discussion

For quantitative analysis, the weighing down should be on the size accuracy, while the contrast and SNR criteria are important for qualitative analysis. Although, the high contrast and SNR are also required in quantitative evaluation as it can assist the detection process by algorithms.

There are not quite agreement between high contrast and SNR, and accurate size of defect. Instead, because the Butterworth filter could balance between image quality and size accuracy, it is suggested for quantitative and qualitative analyses. In addition to, defect detection is also depending on the selection of view which is examined for the specified defect.

For defects in the septal and lateral regions, better results for qualitative and quantitative analysis of these defects will be obtained from the transverse and coronal view of myocardial phantom, respectively. The sagittal view is the best selection for qualitative and quantitative evaluations of defects in the apical and anterior regions.

Totally, in defect size diagrams it could be seen that the size of defect was usually reduced by reduction of the cut-off frequencies. And so, our investigations show that the size of defect could be estimated with a good approximation by use of the introduced equation and imaging protocol. Whereas, some authors in their papers imply that the defect size larger than actual dimension by use of the rotation angle of 180˚ from 45˚ right anterior oblique to 45˚ left posterior oblique that usually use for heart SPECT in the nuclear medicine center[13,14]. Thus, use of the rotation angle of 360˚ could be produced better results for estimation of the defect size in comparison with the routine protocol, which images were recorded over 180˚. Although using of the rotation angle of 180˚ is most popular for cardiac use because they can acquire a study in half the time needed by duration of 360˚.

Some authors have dealt with filters in their literatures in different experimental and phantom study[9,10]. Although most of them have suggested restoration filters such as Wiener and Metz filters as optimal selection[15–17], but these filters have some problematic condition such as; pre-knowing of the point spread function of SPECT system for case study and noise level in the acquired images, as in reference[18] had been studied.

In heart SPECT with rotation angle of 180˚, Van Laerea9 has suggested the use of the Butterworth filter as the best choice between filters, which is also selected filter with rotation angle of 360˚ in our study for quantitative and qualitative evaluation of defect images in different regions of myocardial phantom, but this filter has two variable parameters -cut-off frequency and order- that matching these parameters for acquiring the best image could be more difficult. Thus, with regarding to the obtained results, the Shepp-Logan filter, which is unregarded in the myocardial SPECT, can be used as alternative filter in the heart SPECT study that it has one variable parameter and its optimization in a nuclear medicine center for defect detection is more comfortable.

6. References

1. Germano G. Technical aspect of myocardial SPECT imaging. Journal of Nuclear Medicine. 2001; 42:1499–507.
2. Cullom SJ. Principles of cardiac SPECT. In: DePuey EG, Garcia EV, Berman DS, editors. Cardiac SPECT imaging. USA: Lippincott Williams and Wilkins; 2001.
3. Groch MW, Erwin WD. SPECT in the year 2000: basic principles. Journal of Nuclear Medicine Technology. 2000; 28:233–44.
4. Benoit T, Vivegnis D, Foulon J, Rigo P. Quantitative evaluation of myocardial single photon emission tomographic imaging: application to the measurement of perfusion defect size and severity. European Journal of Nuclear Medicine.1996; 23:1603–12.
5. Kak AC. Image reconstruction from projection. In: Ekstrom M, editor. Digital Image Processing Technique. New York:

. Academic Press; 1984.
6. Kunyansky LA. A new SPECT reconstruction algorithm based on the Nov ikov explicit inversion formula. Inverse Problems. 2001; 17:293–306.
7. Zeniya T, Watabe H, Aoi T, Kim KM, Teramoto N, Hayashi T, Sohlberg A, Kudo H, Iida, H. A new reconstruction strategy for image improvement in pinhole SPECT. European Journal of Nuclear Medicine and Molecular Imaging. 2004; 31:1166–72.
8. Zeng GL. Image reconstruction: a tutorial. Computerized Medical Imaging and Graphics. 2001; 25:97–103.
9. Van Laerea K, Koole M, Lemahieu I, Dierckx R. Image filtering in single-photon emission computed tomography: principles and applications. Computerized Medical Imaging and Graphics. 2001; 25:127–33.
10. Lyra M, Ploussi A. Filtering in SPECT Image Reconstruction. International Journal of Biomedical Imaging. 2011; 1–14.
11. Sadremomtaz A, Taherparvar P. The Influence of filters on the SPECT image of Carlson Phantom. Journal of Biomedical Science and Engineering. 2013; 6(3):291–7.
12. Elkamhawy AA, Chandna H. Minimum detectable defect thickness in SPECT myocardial perfusion test: phantom study with 99mTc and 201Tl. Journal of Nuclear Medicine Technology. 2001; 29(4):183–8.
13. Takavar A, Shamsipour G, Sohrabi M, Eftekhari M. Determination of optimum filter in myocardial SPECT: a phantom study. Iranian Journal of Radiation Research. 2004; 1:205–10.
14. Yusoff MNS, Zakaria A. Determination of the optimum filter for qualitative and quantitative 99mTc myocardial SPECT imaging. Iranian Journal of Radiation Research. 2009; 6(4):173–82.
15. Minoshima S, Maruno H, Yui N, Togawa T, Kinoshita F, Kubota M, Berger KL, Uchida Y, Uno K, Arimizu N. Optimization of Butterworth filter for brain SPECT imaging. Annals Nuclear Medicine.1993; 7:71–9.
16. Manrique A, Hitzel A, Gardin I, Dacher JN, Vera P. Impact of Wiener filter in determining the left ventricular volume and ejection fraction using Thallium-201 gated SPECT. Nuclear Medicine Communications. 2003; 24:907–14.
17. Vakhtangandze T, Hall DO, Zananiri FV, Rees MR. The effect of Butterworth and Metz reconstruction filter on volume and ejection fraction calculations with 99m gated myocardial SPECT. British Journal of Radiology. 2005; 78:733–6.
18. King MA, Schwinger RB. Two dimensional filtering of SPECT images using the Metz and Wiener filters. Journal of Nuclear Medicine. 1984; 25:1234–140.